SENSITIVITY OF TERRESTRIAL CARBON STORAGE TO CO_2-INDUCED CLIMATE CHANGE: COMPARISON OF FOUR SCENARIOS BASED ON GENERAL CIRCULATION MODELS

THOMAS M. SMITH,[1] RIK LEEMANS[2] and HERMAN H. SHUGART
[1] *Department of Environmental Sciences, University of Virginia, Charlottesville, VA 22903, U.S.A.*
[2] *Biosphere Project, International Institute for Applied Systems Analysis, A-2361 Laxenburg, Austria*

Abstract. The potential impacts of CO_2-induced climate change on terrestrial carbon storage was estimated using the Holdridge Life-Zone Classification and four climate change scenarios derived from general circulation models. Carbon values were assigned to life-zones and their associated soils from published studies. All four scenarios suggest an increase in area occupied by forests although details of predicted patterns vary among the scenarios. There is a poleward shift of the forested zones, with an increase in the areal extent of tropical forests and a shift of the boreal forest zone into the region currently occupied by tundra. Terrestrial carbon storage increased from 0.4% (8.5 Gt) to 9.5% (180.5 Gt) above estimates for present conditions. These changes represent a potential reduction of 4 to 85 ppm on elevated atmospheric CO_2 levels.

1. Introduction

At a global scale, the distribution of vegetation is largely controlled by climate. Changes in the global patterns of climate resulting from increased atmospheric CO_2 can potentially change the distribution of terrestrial vegetation. Consequently, carbon flux between the terrestrial biota and the atmosphere will be altered.

A number of studies have used bioclimatic models to examine the potential impacts of climate change on the distribution of major ecosystem complexes at a global scale (Emanuel *et al.*, 1985; Lashof, 1987; Prentice and Fung, 1990). Changes in the distribution of these systems combined with estimates of carbon storage have provided initial estimates of potential changes in terrestrial carbon storage under CO_2-induced climate change (Lashof, 1987; Sedjo and Solomon, 1989; Prentice and Fung, 1990). However, due to differences in the classification models, carbon estimates and spatial resolution of the analyses, it is difficult to compare scenarios (i.e., general circulation models) across studies.

Accordingly, we will examine the potential shifts in major ecosystem complexes and associated carbon storage under four climate change scenarios based on general circulation models (GCMs) using a uniform methodology. In particular, we address the potential of the terrestrial biosphere as a source or sink of carbon under changed climate conditions.

Climatic Change **21**: 367–384, 1992.

2. Methods

The Holdridge Life-Zone Classification (Holdridge, 1967) (Figure 1) is a climate classification scheme relating the distribution of major ecosystem complexes to the climatic variables of biotemperature, mean annual precipitation and the ratio of potential evapotranspiration (PET) to precipitation.

The life-zones are depicted by a series of hexagons in a triangular coordinate system. Two climate variables, biotemperature and annual precipitation, determine the classification. Biotemperature is a temperature sum over a year with the unit temperature values (i.e., average daily, weekly or monthly temperatures) that are used in computing the index set to 0 °C if they are less than or equal to 0 °C.

Identical axes for average annual precipitation form two sides of an equilateral triangle. The potential evapotranspiration (PET) ratio forms the third side, and an axis for mean annual biotemperature is oriented perpendicular to its base. By striking equal intervals on these logarithmic axes, hexagons are formed that designate the Holdridge Life-Zones.

The potential evapotranspiration ratio is the quotient of PET and average annual precipitation. Holdridge (1959) assumes, on the basis of data from several ecosystem types, that PET is proportional to biotemperature (constant of proportionality, 58.93). The PET ratio in the Holdridge Diagram is therefore dependent on the two primary variables, annual precipitation and biotemperature.

One additional division in the Holdridge Classification is based on the occurrence of killing frost. This division is along a critical temperature line that divides hexagons between 12 °C and 24 °C into Warm Temperate and Subtropical Zones. The complete Holdridge Classification at this level includes 37 life-zones.

Expected current distributions of life-zones were mapped using a global climate data base of mean monthly precipitation and temperature at a 0.5° × 0.5° (latitude and longitude) resolution (Leemans and Cramer, 1990). Simulations of current ($1 \times CO_2$) and $2 \times CO_2$ climates from four GCMs (Table I) were used to construct change scenarios. Changes in mean monthly precipitation and temperature were calculated for each GCM scenario for each computational grid element by taking the difference between simulated current and $2 \times CO_2$ climates. Temperatures were expressed as absolute difference ($2 \times CO_2 - 1 \times CO_2$) and precipitation as the ratio of $2 \times CO_2$ to $1 \times CO_2$. These data from each GCM were interpolated to 0.5° × 0.5° using the same technique as applied in the development of the database for current climate (Leemans and Cramer, 1990). The technique used was a triangulation of all datapoints (algorithm developed by Green and Sibson, 1978) followed by a smooth surface fitting (Akima, 1978). Changes in monthly precipitation and temperature were then applied to the global climate data base to provide a change scenario. The altered data bases corresponding to each of the four GCM scenarios were then used to reclassify the grid cells (0.5° × 0.5°) using the Holdridge Classification.

To determine the effects of the climate change scenarios on patterns of global

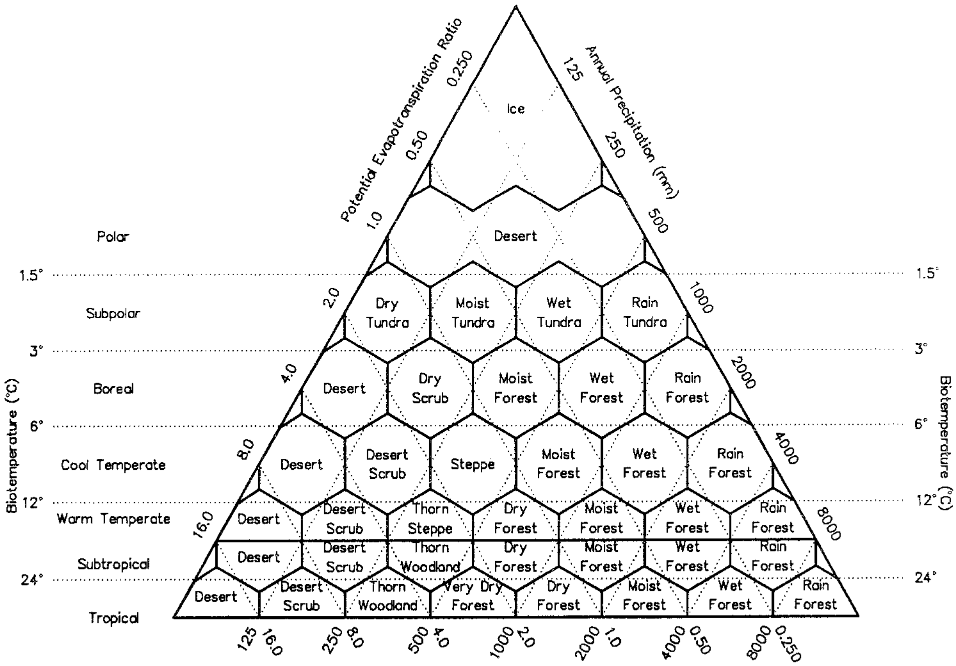

Fig. 1a. Holdridge climate-vegetation classification scheme (from Holdridge 1967).

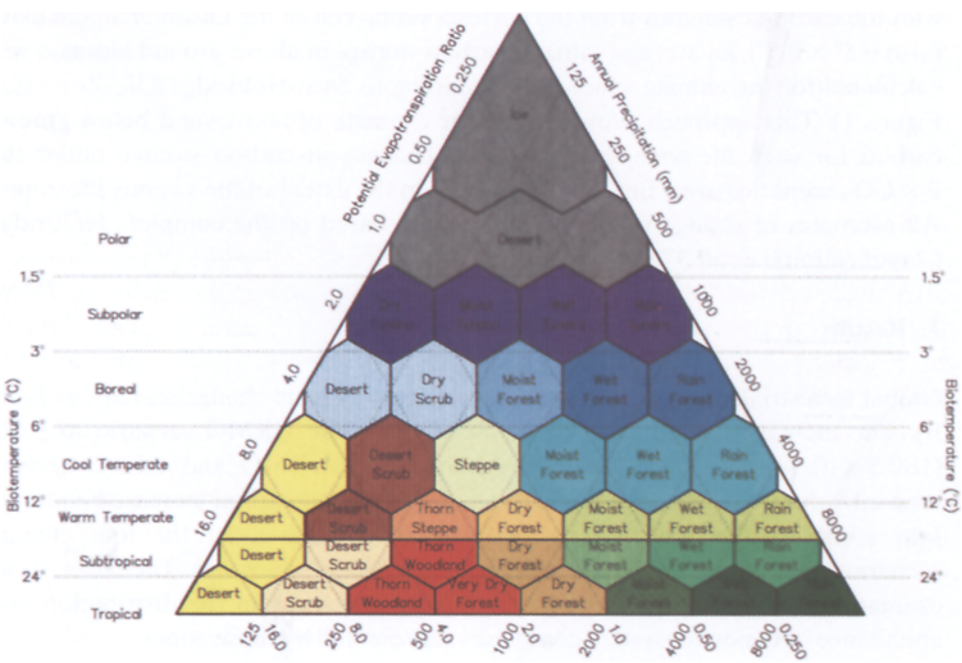

Fig. 1b. Color key to aggregation scheme used in Figures 2–6.

TABLE I: General circulation models used to construct climate change scenarios

GCM	Resolution (lat/lon)	Change in mean global:	
		Temperature (°C)	Precipitation (%)
[1]Oregon State University (OSU)	4 × 5°	2.84	7.8
[2]Geophysical Fluid Dynamics Laboratory (GFDL)	4.5 × 7.5°	4.00	8.7
[3]Goddard Institute for Space Studies (GISS)	7.8 × 10°	4.20	11.0
[4]United Kingdom Meteorological Office (UKMO)	5 × 7.5°	5.20	15.0

carbon storage, each of the 37 Holdridge Life-Zones was assigned a value for carbon in both above-ground biomass and soil. Soil carbon estimates for the Holdridge Life-Zones were taken directly from Post *et al.* (1982). Estimates of carbon in above-ground biomass for each life-zone were calculated using data from Olson *et al.* (1983). Olson *et al.* (1983) does not classify ecosystems according to the Holdridge Life-Zone system, therefore it was necessary to estimate carbon values for the life-zones directly from the climate variables used in the Holdridge Life-Zone Classification (i.e., biotemperature and annual precipitation). Combining the biotemperature and annual precipitation data for each 0.5° × 0.5° cell with the carbon estimates from the corresponding cell of the Olson *et al.* database (also 0.5° × 0.5°), an average value of carbon storage in above-ground biomass was calculated for the climate space corresponding to each Holdridge Life-Zone (see Figure 1). This approach provides a single estimate of above- and below-ground carbon for each life-zone, and therefore, changes in carbon storage under the 2 × CO_2 scenarios are a function of changes in the extent of the various life-zones. All estimates of change in carbon storage are based on the complete Holdridge Classification (i.e., all 37 life-zones).

3. Results

Global terrestrial carbon increased under all four climate change scenarios (Table II). The increase ranged from 0.4% (8.5 Gt) for the UKMO scenario to 9.5% (180.5 Gt) for the OSU scenario. Although the UKMO and GFDL derived scenarios show a decrease in soil carbon; above-ground carbon increased under all four scenarios. The changes in total carbon storage under the four climate scenarios correspond to shifts in the areal coverage of life-zones. Therefore, these estimates are best interpreted by examining the changes in the distribution and abundance of major ecosystem complexes represented by those zones.

Maps of predicted global life-zone distribution under current climate and the four GCM climate change scenarios are shown in Figures 2–6. The life-zones have

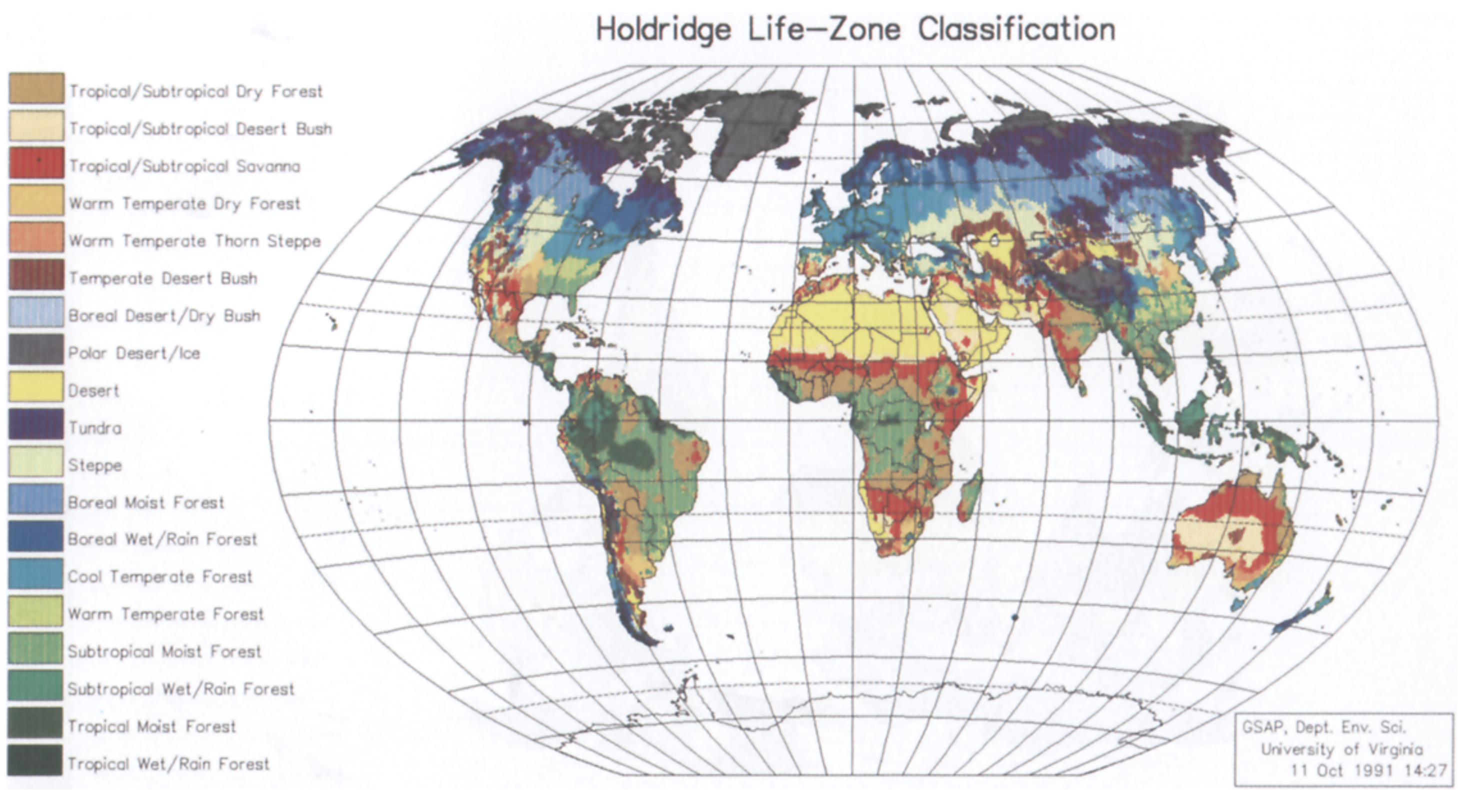

Fig. 2. Global map of Holdridge Life-Zones under current climate conditions. The resolution is 0.5° latitude × 0.5° longitude. Key relating aggregated classes to life-zone is shown in Figure 1.

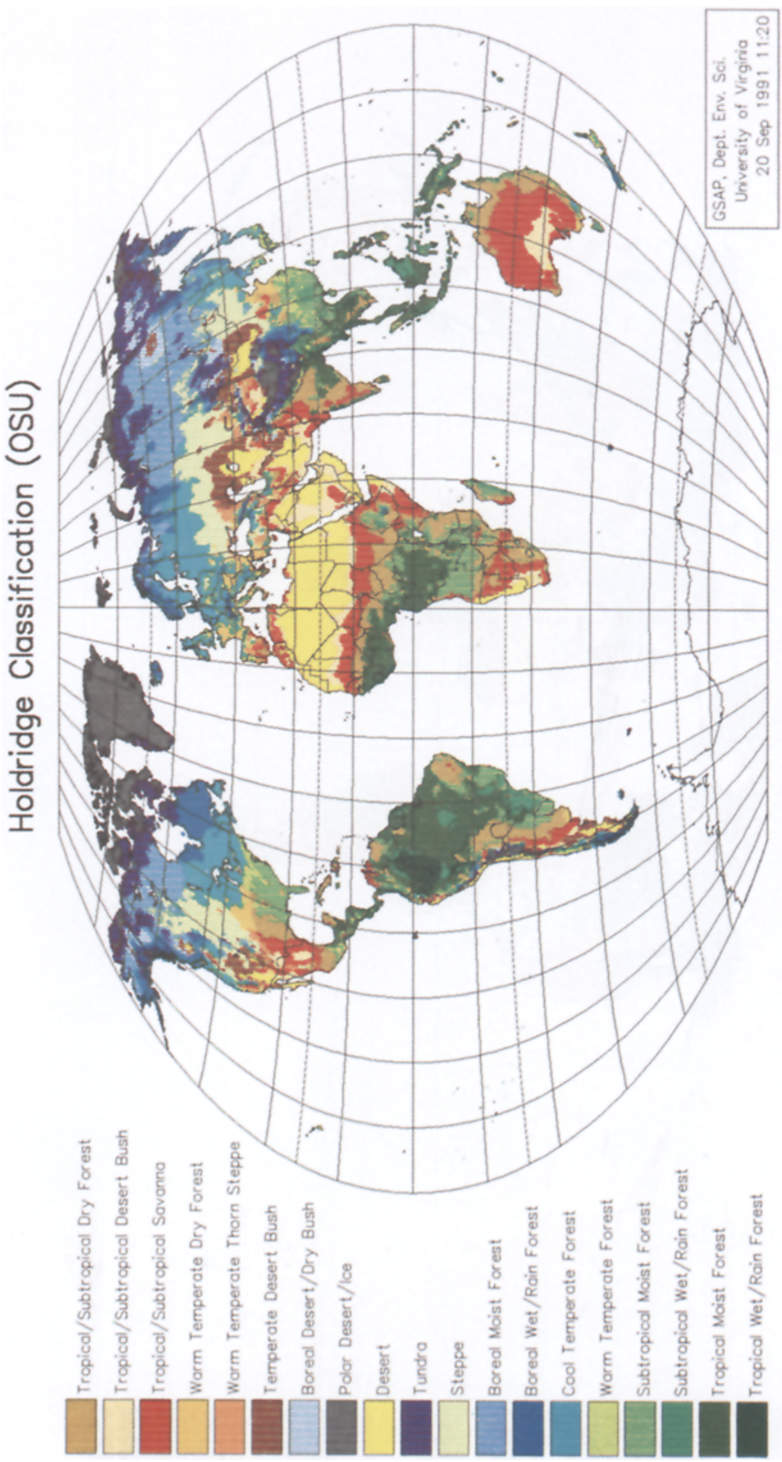

Fig. 3. Global map of Holdridge Life-Zones under the OSU-derived climate change scenario (Table 1). Key relating aggregated classes to life-zones is shown in Figure 1.

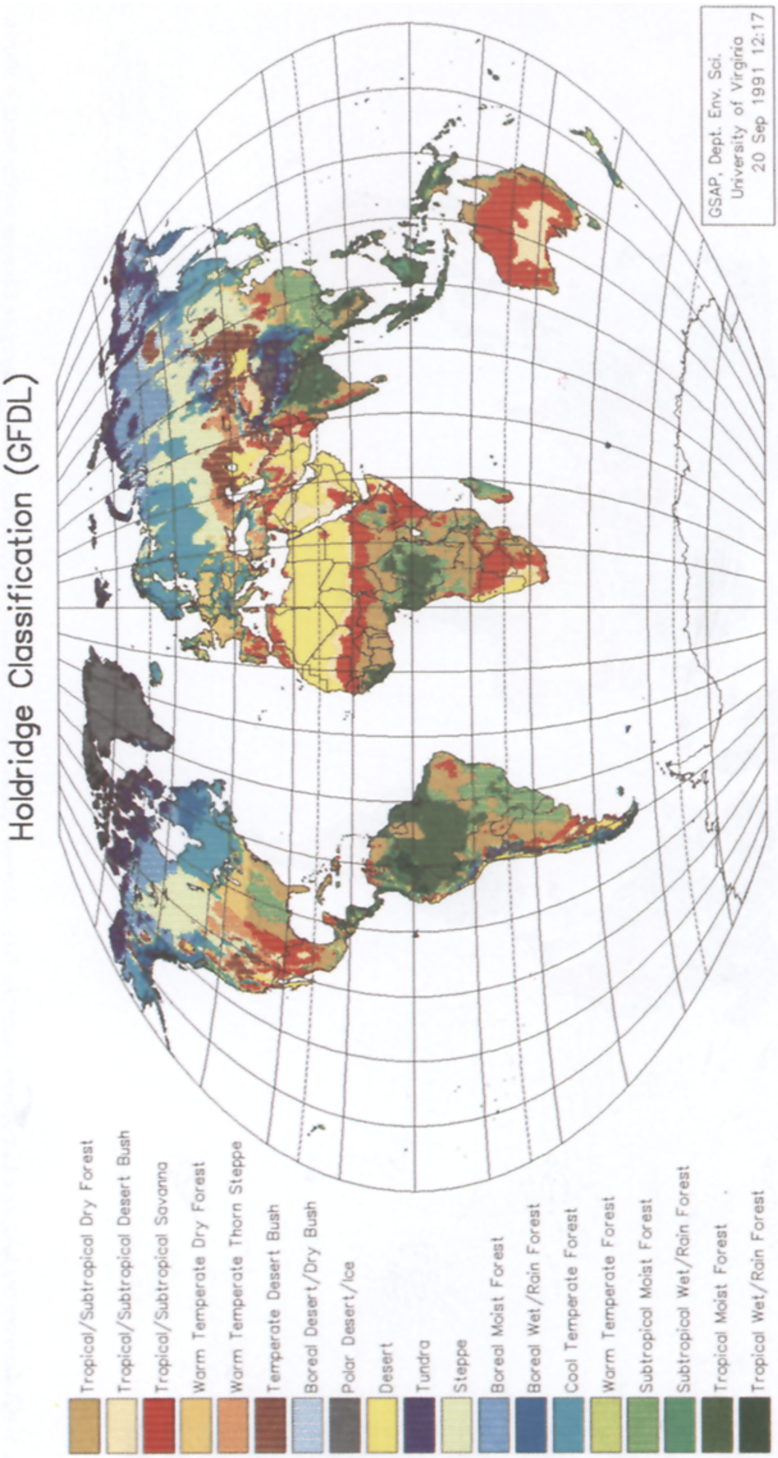

Fig. 4. Global map of Holdridge Life-Zones under the GFDL-derived climate change scenario (Table I). Key relating aggregated classes to life-zones is shown in Figure 1.

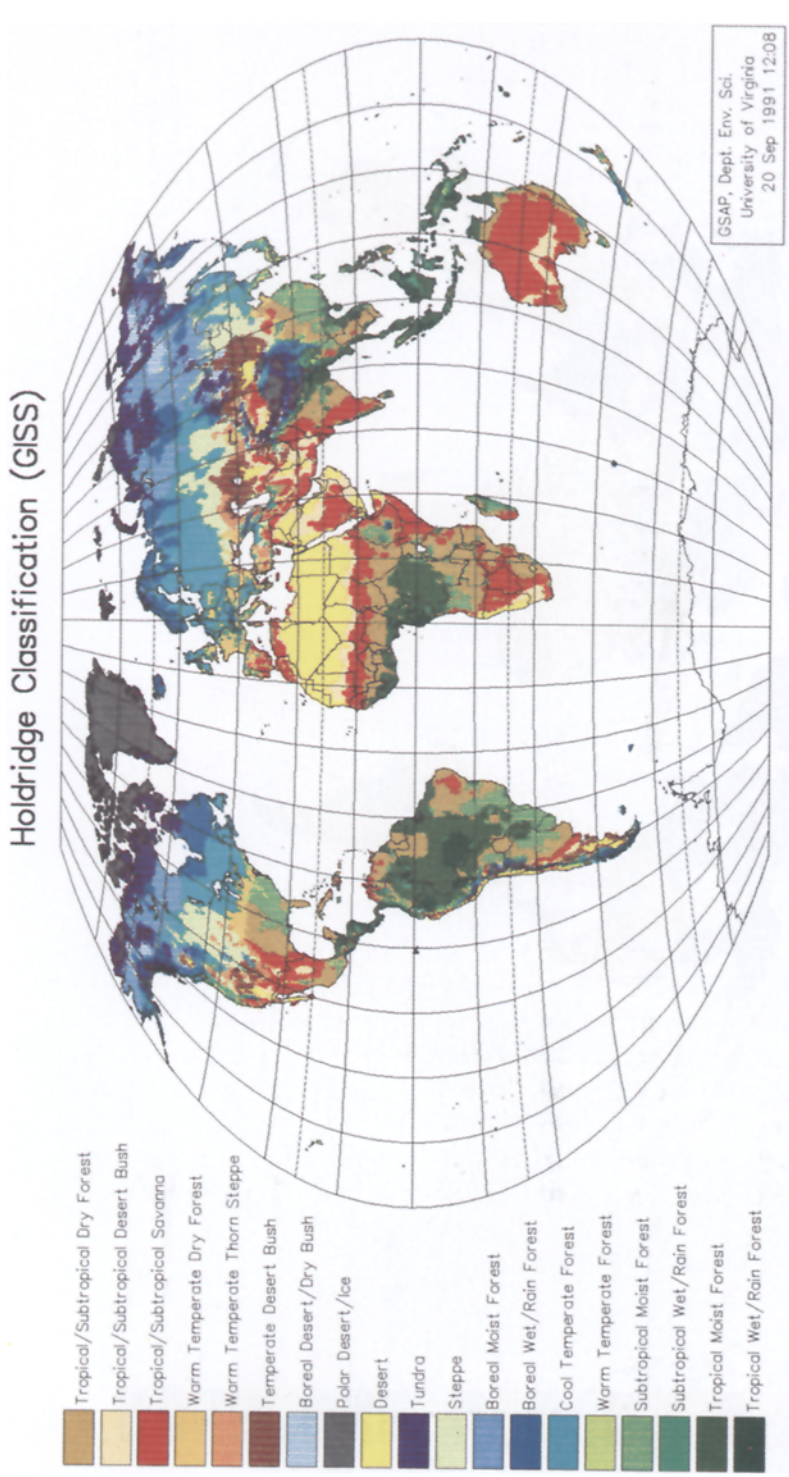

Fig. 5. Global map of Holdridge Life-Zones under the GISS-derived climate change scenario (Table I). Key relating aggregated classes to life-zones is shown in Figure 1.

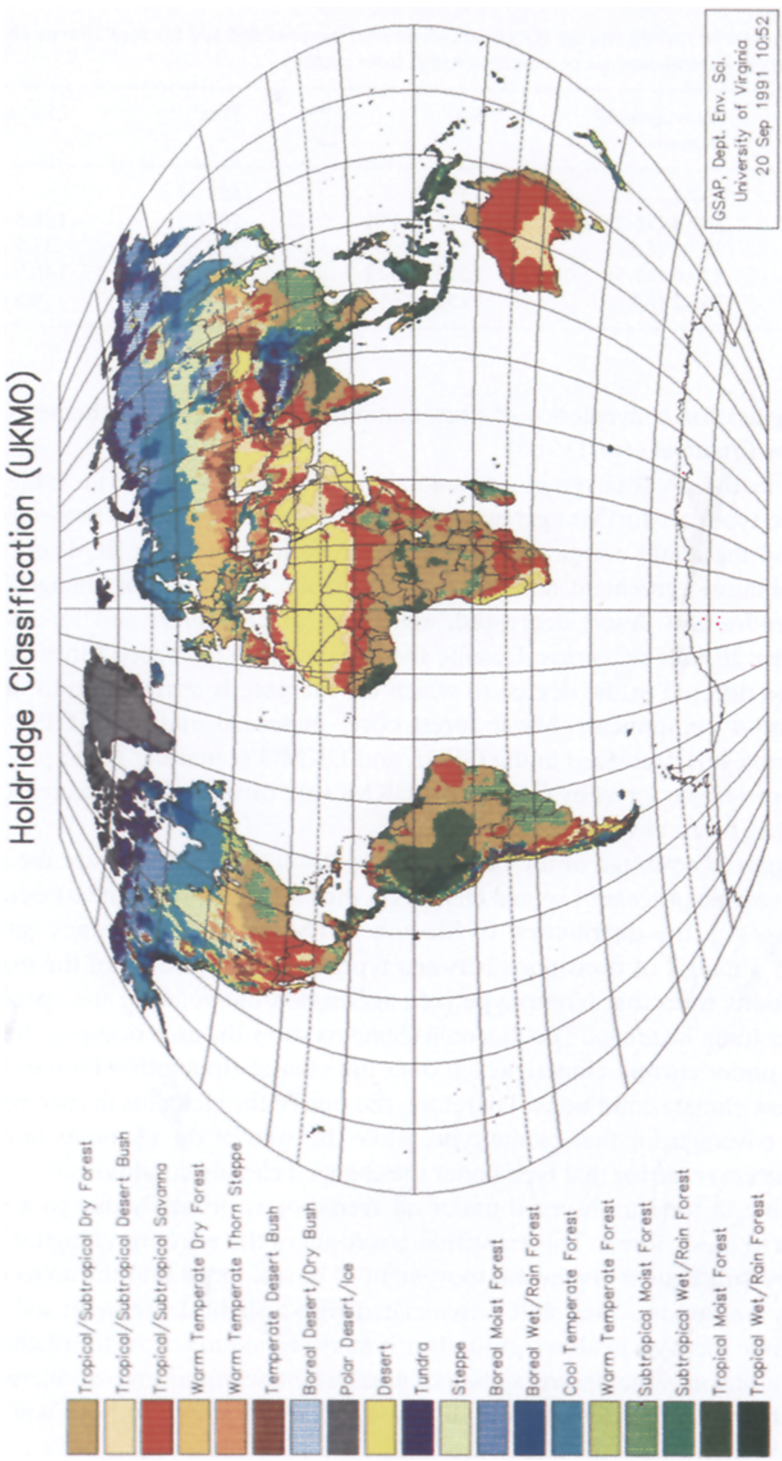

Fig. 6. Global map of Holdridge Life-Zones under the UKMO-derived climate change scenario (Table I). Key relating aggregated classes to life-zones is shown in Figure 1.

TABLE II: Changes in carbon storage (Gt) in above-ground biomass and soil for four climate change scenarios. Values in parentheses are percentage change from current

Scenario	Aboveground Biomass	Soil	Total	Change
Current	737.2	1158.5	1895.7	
OSU	860.4 (16.7)	1215.8 (4.9)	2076.2	180.5 (9.5)
GFDL	782.3 (6.1)	1151.3 (−0.6)	1933.6	37.9 (2.0)
GISS	829.6 (12.5)	1213.0 (4.7)	2042.6	146.9 (7.7)
UKMO	765.2 (3.8)	1139.0 (−1.7)	1904.2	8.5 (0.4)

been aggregated for convenience of presentation. The aggregation scheme is the same used by Emanuel *et al.* (1985).

Changes in the areal coverage of major biome-types are shown in Table III. These biome-types are further aggregates of the Holdridge Life-Zones presented in Figure 1, and the zones comprising the types are defined in Table III. There is a general qualitative agreement among scenarios in the directions of change. The extent of tundra and desert decreased, and those of grasslands and forests increased under all four scenarios. Despite the agreement in increased forest cover, the scenarios differed in the degree to which the increase is attributable to mesic and xeric forest components. Mesic forest cover increased under the GISS and OSU scenarios, but decreased in the GFDL and UKMO scenarios. These predicted decreases in mesic forest by GFDL and UKMO are offset by larger increases in dry forest, thus forest cover increased overall.

The changes in coverage of the biome-types presented in Table III are the outcome of a dynamic process of spatial changes in the climate pattern, and associated spatial changes in the distribution of life-zones. These spatial dynamics can be described as a matrix of transitions between types (Table IV). Rows of the matrix show transitions from that biome-type (i.e., aggregated life-zone) to the specified type in the column headings. The diagonal elements show the area occupied by the biome-type under current climate which does not change (to another biome-type) under the new climate conditions. Therefore, the sum of the elements in each row is the current coverage for that biome-type, while the sum of the elements in each column is the coverage for that type under the changed climate conditions.

The decline in tundra observed under all scenarios is primarily due to a shift from tundra to mesic forest. This transition is a result of the warming at higher latitudes and the subsequent northward movement of boreal forest into the areas now occupied by wet tundra. This shift is associated with a slight decrease in soil carbon, but a large increase in above-ground carbon. A second major vector of change in the tundra region is the desertification of areas where warming and/or decreases in precipitation occurs, resulting in a decrease in carbon stored in both soil and above-ground biomass.

The decrease in the global extent of desert seen in all four scenarios is a function

TABLE III: Changes in the areal coverage of major biome-types* under current and changed climate conditions

	Current area ($km^2 \times 10^3$)	OSU	GFDL	GISS	UKMO
Tundra	939	−302	−515	−314	−573
Desert	3699	−619	−630	−962	−980
Grassland	1923	380	969	694	810
Dry Forest	1816	4	608	487	1296
Mesic Forest	5172	561	−402	120	−519

* Tundra: Polar Dry Tundra, Polar Moist Tundra, Polar Wet Tundra, Polar Rain Tundra
Desert: Polar Desert, Boreal Desert, Cool Temperate Desert, Warm Temperate Desert, Subtropical Desert, Subtropical Desert Bush, Tropical Desert, Tropical Desert Bush
Grassland: Cool Temperate Steppe, Warm Temperate Thorn Steppe, Subtropical Thorn Steppe, Tropical Thorn Steppe, Tropical Very Dry Forest
Dry Forest: Warm Temperate Dry Forest, Subtropical Dry Forest, Tropical Dry Forest
Mesic Forest: Moist, Wet and Rain Forest for Boreal, Cool Temperate, Warm Temperate, Subtropical and Tropical temperature Zones

of the shift from desert to tundra in the higher latitudes, and from desert to grassland in the temperate and tropical regions. Furthermore, there is a significant conversion from desert to mesic forest under the GFDL and UKMO scenarios. These shifts occur in the northern latitudes where cold desert/dry tundra zones increase in both temperature and precipitation. All shifts from desert to other biome-types represent a net increase in stored carbon (both soil and above-ground).

The increased cover of grassland under all scenarios is a function of both shifts from desert to grassland with increased precipitation in areas of the temperate and tropical regions, and the transition of dry and mesic forests to grassland as a result of drying in all forested regions. These shifts represent both an increase and decrease in carbon storage. Potential carbon storage increases in the transition from desert to grassland, but decreases significantly with the transition from forest to grassland.

The extent of dry forest increases with increasing precipitation in grassland regions, and with increased temperatures and/or decreased precipitation in mesic forests. The latter transition occurs primarily in the subtropical and tropical regions and represents a large decrease in carbon in all scenarios. This transition is the largest in the UKMO scenario, resulting in a doubling of the global extent of dry forest.

The major transition towards mesic forest is the shift from tundra to boreal forest discussed earlier. This transition is followed in importance by the shift from dry to mesic forest, primarily in the subtropical and tropical regions. The extent of the transition from tundra to boreal forest is similar (ranging from 638.3 to 771.6 $km^2 \times 10^3$) for the four scenarios. The major difference between the scenarios in the predicted areal coverage of mesic forest is the degree of mesic forest decline

TABLE IV: Transition matrices for the four GCM-based climate change scenarios. Matrices show the changes in coverage between biome-types. Values are in km^2 × 10^3 (T – Tundra; D – Desert; G – Grassland; DF – Dry Forest; MF – Mesic Forest)

OSU	To:	T	D	G	DF	MF	Total
From:	T	189.3	111.3			638.3	938.6
	D	447.9	2869.6	372.7		8.9	3699.1
	G		60.0	1565.2	295.8	2.1	1923.1
	DF			59.3	1282.3	474.1	1815.7
	MF		14.6	306.1	242.3	4609.2	5172.2
	Total	637.2	3055.5	2303.3	1820.4	5732.6	

GFDL	To:	T	D	G	DF	MF	Total
From:	T	18.5	177.6	29.2	0.2	713.3	938.8
	D	405.2	2784.1	337.8	0.3	171.8	3699.2
	G		67.9	1663.4	181.0	10.8	1923.1
	DF			141.8	1490.8	183.2	1815.8
	MF		9.2	720.6	751.9	3690.6	5172.3
	Total	423.7	3038.8	2892.8	2424.2	4769.7	

GISS	To:	T	D	G	DF	MF	Total
From:	T	167.4	114.5	2.1		655.0	939.0
	D	456.7	2559.5	617.0	5.4	60.5	3699.1
	G		33.8	1645.3	198.2	45.7	1923.0
	DF			152.9	1427.2	235.6	1815.7
	MF		5.3	200.0	672.0	4295.2	5172.5
	Total	624.1	2713.1	2617.3	2302.8	5292.0	

UKMO	To:	T	D	G	DF	MF	Total
From:	T	20.5	110.3	35.3	1.2	771.6	938.9
	D	343.9	2505.1	566.9	4.1	278.7	3698.7
	G	0.5	37.8	1520.4	353.8	10.5	1923.0
	DF	0.3	5.8	211.7	1374.7	223.3	1815.8
	MF	0.3	25.7	399.0	1378.3	3369.0	5172.3
	Total	365.5	2684.7	2733.3	3112.1	4653.1	

associated with drying in the subtropical and tropical regions (i.e., the shift to dry forest discussed above).

Mesic forests are by far the largest component of terrestrial carbon storage, currently covering 38% of the land surface and containing 58% of the total carbon storage (i.e., soil and above-ground). Changes in areal coverage of the five major mesic forest types as defined by Holdridge are presented in Figure 7. The types are defined by summing over the moist, wet and rain forest life-zones for each tem-

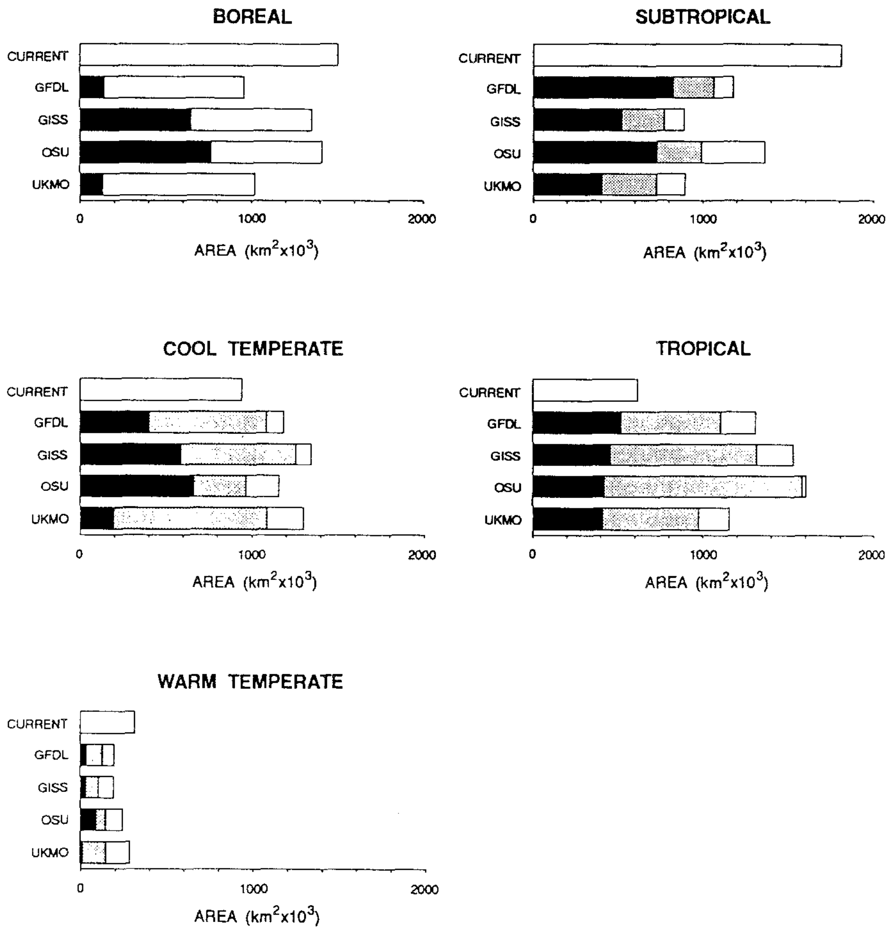

Fig. 7. Areal coverage of mesic forest types under current climate and four climate change scenarios.

Black: Area which is currently occupied by that forest type and remains so under the changed climate conditions (i.e., stable).

Grey: Area which is predicted to change to that forest type but is currently occupied by some other forest type.

Unshaded: Area which is predicted to change to that forest type but is not currently occupied by mesic forest (i.e., tundra, grassland, etc.).

perature zone (see Figure 1). The histograms present the areas for each forest type under current climate and the four climate change scenarios. These predicted changes in coverage under the scenarios can be examined in terms of their components. The portion of the histogram shaded black represents the area of the given forest type that does not change type under the scenario. The grey portion represents the area which was covered by some other mesic forest type under current climate conditions, but is predicted to change to that forest type under the new climate conditions. The unshaded portion is that area which is predicted to change to that forest type but is currently covered by a non-mesic forest type (i.e., dry forest, grassland, desert or tundra).

The areal cover of tropical forest increased under all scenarios, from 87% for the UKMO scenario to 159% for OSU. This increase is largely due to the reclassification to tropical forest of areas which are currently occupied by subtropical and warm temperate forest. This shift is due to the overall warming predicted by the GCM's and the subsequent expansion of the tropical zone as defined by biotemperature in the Holdridge model (Figure 1). Of the areas predicted to change to tropical forest under the climate change scenarios, 74 to 98% are currently occupied by another mesic forest type. This shift to warmer forest types is accompanied by a significant increase in above-ground carbon.

In general, the global warming results in a poleward shift in all forest zones with the subsequent expansion of the boreal forest zone into the region currently occupied by tundra. This poleward shift can be seen in Figure 7, where the majority of the area involved in the spatial shifts in forest type (with the exception of boreal forest) are from areas currently occupied by other mesic forest types (i.e., grey area of histograms).

4. Discussion

The four scenarios considered in this study all suggest a potential increase in terrestrial carbon storage with an associated reduction in atmospheric CO_2 levels from concentrations used in the $2 \times CO_2$ GCM simulations. These potential reductions range from 4 to 85 ppm. The increase in carbon storage is primarily due to the: (1) poleward shift of the forest zones, with an increase in the extent of tropical forest and a northern movement of the boreal forest zone into areas currently occupied by tundra, and (2) a decrease in the global extent of desert. These findings differ from those of earlier studies which have examined the impacts of CO_2-induced climate change on global carbon storage.

Emanuel *et al.* (1985) used the Holdridge Life-Zone Classification (Holdridge, 1967) to map the global distribution of terrestrial ecosystem complexes under present climate conditions as well as under a scenario of climate change resulting from increasing atmospheric concentrations of CO_2 (Manabe and Stouffer, 1980). The largest changes occurred in the higher latitudes where boreal forest was replaced by more temperate complexes. Changes in the tropics were smaller with some shift from moist to dry forest. In general, the changes resulted in a decrease in the total extent of forested area with a corresponding decline in above-ground biomass/carbon storage (Sedjo and Solomon, 1989). These results were largely influenced by the fact that the study considered changes in temperature only. The increased temperature combined with current patterns of precipitation resulted in a general drying of the more mesic forested regions.

Lashof (1987) developed a classification system of 14 ecosystem types based on the vegetation classification of Olson *et al.* (1983). The global distribution of these types were then related to mean winter and summer temperature and precipitation. The resulting model was used to examine potential shifts in the distribution of ecosystems and associated changes in terrestrial carbon storage under climate change scenarios from the National Center for Atmospheric Research (NCAR) (Washington and Meehl, 1984), Geophysical Fluid Dynamics Laboratory (GFDL) (Wetherald and Manabe, 1986) and Goddard Institute for Space Studies (GISS) (Hansen *et al.*, 1984) general circulation models.

The results for the GISS scenario were in qualitative agreement with the current study, with carbon storage increasing by 28 Gt. In contrast, carbon storage declined in both the GFDL (−64 Gt) and NCAR (−40 Gt) scenarios. Soil carbon declined under all three scenarios as a result of the transition from boreal forest to grassland. For the GISS scenario, this decrease was offset by a significant increase in forest cover in the tropics. Above-ground carbon decreased in the other two scenarios as a result of forest decline in the warm temperate, subtropical and tropical zones.

The differences between patterns reported by Lashof and those found in this study are due in large part to the limited number of ecosystem types in the Lashof classification. The absence of a transition type between warm grasslands and dry forest led to an abrupt shift (and associated decrease in carbon storage) with decreased precipitation in areas of dry forest. Similarly, the use of only a single boreal forest type (as compared to three in Olson *et al.* (1983) and Holdridge (1967)) resulted in a much larger shift from forest to grassland in the boreal zone than predicted in our analyses.

In addition, the use of only a single class for warm-humid forest resulted in an insufficient description of the range of forest types and associated carbon values for the warm temperate, subtropical and tropical region. The large range of climate space encompassed by this single forest class resulted in an underestimation of current tropical forest cover (e.g., absence of Amazonian forest) as well as an anomalous response to patterns of precipitation change in subtropical and tropical regions. Decreases in precipitation led to a shift from humid to dry forest, however, increased precipitation (i.e., warmer and wetter conditions) resulted in no change in productivity and carbon storage in currently forested areas.

Prentice and Fung (1990) used a modified version of the Holdridge Classification (Prentice, 1990) to examine the impacts of perturbed climates on the distribution of global vegetation and associated changes in terrestrial carbon. Using predicted climate patterns from the Goddard Institute for Space Studies (GISS) general circulation model (Hansen *et al.*, 1988) for conditions of $2 \times CO_2$, Prentice and Fung found a 235 Gt increase in terrestrial carbon storage, resulting in a strong negative feedback on elevated atmospheric CO_2 (128 ppm). The increase in carbon storage was primarily associated with a large increase (75%) in the extent of tropical rainforest under the changed climate conditions.

Although the present study found a similar expansion of tropical forests for the GISS derived scenario (79%), the associated increases in carbon were considerably less (147 Gt). As with the Lashof study, this discrepancy is most likely to be due to a difference between the classification schemes, particularly in the tropical realm. Prentice and Fung aggregate vegetation units into 14 types as compared to the 37 types of the Holdridge Classification used in this study. The greater number of categories used in this study results in a more gradual change in biomass and soil carbon values with changes in precipitation and temperature. This gradient is particularly pronounced in the warm temperate, subtropical and tropical regions where the shifts between Holdridge Life-Zones do not result in as much change in carbon as in the modified system of Prentice and Fung. However, despite these differences, both studies agree on the general trends of vegetation pattern and carbon dynamics.

Despite the qualitative agreement among scenarios, the results discussed above must be viewed in light of the limitation of the methodology. As with any classification scheme, the Holdridge model is an abstraction of the actual vegetation pattern. The Holdridge Life-Zone model is a climate classification rather than a classification based on actual vegetation distribution, such as the system developed by Box (1981). Secondly, the limited number of categories of vegetation or biome-types and the fixed carbon values within a type results in a coarse resolution of carbon dynamics. In reality, vegetation pattern (i.e., physiognomic structure, species composition and biomass) and carbon values vary within any one life-zone or classification unit. This level of variation may not dramatically influence estimates of current carbon storage if estimated mean values for each of the zones are reasonable. However, this discrete view of vegetation pattern results in a threshold phenomenon when applying change scenarios. Carbon values for a grid cell will not vary with climate until the climate varies beyond the boundary conditions of the zone to which the cell is classified. As such, the dynamics are inherently scaled to the classification scheme, and the more aggregated the scheme, the more pronounced the threshold effect.

The approach also assumes that the vegetation unit or biome-structure moves as a fixed unit in time and space. This assumption may not hold, especially under conditions where the changed climate has no current analogue.

The Holdridge Classification, like all climate-vegetation classification models, is correlative and based on a limited set of variables. Although the bioclimatic indices used in the classification may do a sufficient job of bounding present vegetation patterns, the actual patterns are a function of additional factors not explicitly considered in the model (e.g., soils) which may vary differently (both temporally and spatially) under the changed climate conditions.

Perhaps most importantly, the results represent equilibrium solutions for both climate (i.e., $2 \times CO_2$) and vegetation dynamics. In reality, the vegetation would most likely be unable to track the true transient climate dynamic. Although changes in the climate pattern as suggested by the GCM simulations may occur on a timescale of decades to a century, the response of vegetation and soils to those changes may occur at different and varying timescales. In areas where biomass values decrease due to moisture stress (i.e., higher PET ratio) the changes may occur quickly as the environmental conditions become such that the present vegetation can no longer be supported (e.g., forest to grassland).

In contrast, increases in biomass may require much longer periods of time. In some cases the present vegetation may show increased growth or recruitment under the more favorable conditions. However, major shifts of forest type (e.g., warm temperate to tropical rainforest, or boreal to cool temperate forest) are dependent on the movement of species across the landscape and the ability of new species to invade existent communities. These changes in forest type would operate on timescales related to the lifecycle or longevity of the component species. In the case of many forest species this may be on the order of centuries.

Changes in soil carbon may require longer periods of time to track changes in climate conditions. This difference in the timescale associated with vegetation and soil response to changing climate could have a major influence on the temporal dynamics of carbon flux between atmospheric and terrestrial pools. If changes in soil carbon are slow in comparison to vegetation, the initial differences between the scenarios may not be as great as expected under the combined estimates carbon storage in soil and above-ground vegetation (Table II). All scenarios predict an increase in above-ground biomass, however, the scenarios differ in their predictions for soil carbon. The GFDL and UKMO predict a decline in soil carbon while the GISS and OSU scenarios predict an increase. It is this divergence in patterns of soil carbon which account for the large differences between scenarios in total carbon.

The lag between climate and soils may also have a major influence of changes in vegetation response, especially in those areas where predicted transitions would be dependent on large scale changes in the current soil conditions (e.g., polar desert-tundra-boreal forest transitions).

The transient dynamic, of both climate and vegetation, will require a linked climate-terrestrial biosphere model. However, the present study provides a qualitative index of change and a means of comparing an array of scenarios with a single methodology. The general pattern of results across scenarios suggests a qualitative agreement among the GCM models with respect to the direction of change at a global scale despite their quantitative differences in climate pattern.

Acknowledgements

The authors would like to thank W. R. Emanuel, A. Solomon and W. Cramer for helpful discussion during the development of the manuscript. Research was supported by the Environmental Protection Agency's Office of Policy, Planning and Evaluation under grant CR816267, and the Biosphere Project of the International Institute for Applied Systems Analysis, Laxenburg, Austria.

References

Akima, H.: 1978, 'A Method of Bivariate Interpolation and Smooth Surface Fitting for Irregular Disturbed Datapoints', *ACM Trans. Math. Software* **4**, 148–159.

Box, E. O.: 1980, *Macroclimate and Plant Forms: An Introduction to Predictive Modeling in Phytogeography*, Junk, The Hague.

Emanuel, W. R., Shugart, H. H. and Stevenson, M. P.: 1985, 'Climatic Change and the Broad-Scale Distribution of Terrestrial Ecosystem Complexes', *Climatic Change* 7, 29–43.

Green, P. J. and Sibson, R.: 1978, 'Computing Dirichlet Tessellations in the Plane', *The Computer Journal* **21**, 168–173.

Hansen, J., Lacis, A., Rind, D., Russell, G., Stone, P., Fung, I., Reudy, R. and Lerner, J.: 1984, 'Climate Sensitivity: Analysis of Feedback Mechanisms', in Hansen, J. and Thompson, R. (eds.), Geophysical Monogr. 29, American Geophysical Union, Washington, D.C.

Hansen, J., Fung, I., Lacis, A., Rind, D., Russell, G., Lebedeff, S., Reudy, R. and Stone, P.: 1988, 'Global Climate Changes as Forecast by the GISS-3-D Model', *J. Geophys. Res.* **93**, 9341–9364.

Holdridge, L. R.: 1959, 'Simple Method for Determining Potential Evapotranspiration from Temperature Data', *Science* **130**, 572.

Holdridge, L. R.: 1967, *Life Zone Ecology*, Tropical Science Center, San Jose.

Lashof, D. A.: 1987, *The Role of the Biosphere in the Global Carbon Cycle: Evaluating Through Biospheric Modeling and Atmospheric Measurement*, Ph.D. dissertation, University of California, Berkeley.

Leemans, R. and Cramer, W.: 1990, 'The IIASA Climate Database for Land Area on a Grid of 0.5° Resolution', WP-41, International Institute for Applied Systems Analysis, Laxenburg.

Manabe, S. and Stouffer, R. J.: 1980, 'Sensitivity of a Global Climate Model to an Increase in CO_2 Concentration in the Atmosphere', *J. Geophys. Res.* **85**, 5529–5554.

Manabe, S. and Wetherald, R. T.: 1987, 'Large Scale Changes in Soil Wetness Induced by an Increase in Carbon Dioxide', *J. Atm. Sci.* **44**, 1211–1235.

Mitchell, J. F. B.: 1983, 'The Seasonal Response of a General Circulation Model to Changes in CO_2 and Sea Temperatures', *Q. J. Roy. Met. Soc.* **109**, 113–152.

Olson, J. S., Watts, J. A. and Allison, L. J.: 1983, 'Carbon in Live Vegetation of Major World Ecosystems', ESD Pub. No. 1997, Oak Ridge National Laboratory, TN.

Post, W. M., Emanuel, W. R., Zinke, P. J. and Stangenberger, A. G.: 1982, 'Soil Carbon Pools and World-Life Zones', *Nature* **298**, 156–159.

Prentice, K. C. and Fung, I. Y.: 1990, 'Bioclimatic Simulations Test the Sensitivity of Terrestrial Carbon Storage to Perturbed Climates', *Nature* **346**, 48–51.

Prentice, K. C.: 1990, 'Bioclimatic Distribution of Vegetation for GCM Studies', *J. Geophys. Res.* (in press).

Schlesinger, M. and Zhao, Z.: 1988, 'Seasonal Climatic Changes Induced by Doubled CO_2 as Simulated by the OSU Atmospheric GCM/Mixed Layer Ocean Model', Oregon St. U., Corvallis, OR, Climate Research Institute.

Sedjo, R. A. and Solomon, A. M.: 1989, 'Climate and Forests', in Rosenberg, N. J., Easterling, W. E., Crosson, P. R. and Darmstadter, J. (eds.), *Greenhouse Warming: Abatement and Adaptation*, Resources For The Future, Washington, D.C.

Washington, W. and Meehl, J.: 1984, 'Seasonal Cycle Experiments on the Climate Sensitivity due to a Doubling of CO_2 with an Atmospheric General Circulation Model Coupled to a Simple Mixed Layer Ocean Model', *J. Geophys. Res.* **89**, 9475–9503.

Wetherald, R. and Manabe, S.: 1986, 'An Investigation of Cloud Cover Change in Response to Thermal Forcing', *Climatic Change* **8**, 5–23.

(Received 3 December, 1990; in revised form 3 October, 1991)